| 1 Report No | 2 Government Accession No | 3 Recipient's Catalog No |
|---|---|---|
| NASA TM X-3482 | | |

| 4 Title and Subtitle | 5 Report Date |
|---|---|
| COLD-AIR INVESTIGATION OF A $3\frac{1}{2}$-STAGE FAN-DRIVE TURBINE WITH A STAGE LOADING FACTOR OF 4 DESIGNED FOR AN INTEGRAL LIFT ENGINE<br>II - PERFORMANCE OF 2-, 3-, AND $3\frac{1}{2}$-STAGE CONFIGURATIONS | February 1977 |
| | 6 Performing Organization Code |
| 7 Author(s)<br>Warren J. Whitney, Harold J. Schum, and Frank P. Behning | 8 Performing Organization Report No<br>E-8874 |
| | 10 Work Unit No<br>505-04 |
| 9 Performing Organization Name and Address<br>Lewis Research Center<br>National Aeronautics and Space Administration<br>Cleveland, Ohio 44135 | 11 Contract or Grant No |
| | 13 Type of Report and Period Covered<br>Technical Memorandum |
| 12 Sponsoring Agency Name and Address<br>National Aeronautics and Space Administration<br>Washington, D.C. 20546 | 14 Sponsoring Agency Code |

15 Supplementary Notes

16 Abstract

The stage work distribution among the three stages was very close to the design value. The specific work output-mass flow characteristics of the three stages were closely matched. The efficiency of the $3\frac{1}{2}$-stage turbine at design specific work output and design speed was within 0.008 of the estimated value, and this agreement was felt to demonstrate the adequacy of the prediction method in the high stage loading factor regime.

| 17. Key Words (Suggested by Author(s)) | 18. Distribution Statement |
|---|---|
| Axial flow turbines<br>Turbofan engines | Unclassified - unlimited<br>STAR Category 07 |

| 19. Security Classif. (of this report) | 20. Security Classif. (of this page) | 21. No of Pages | 22 Price* |
|---|---|---|---|
| Unclassified | Unclassified | 27 | A03 |

* For sale by the National Technical Information Service, Springfield, Virginia 22161

# COLD-AIR INVESTIGATION OF A $3\frac{1}{2}$-STAGE FAN-DRIVE TURBINE WITH A STAGE LOADING FACTOR OF 4 DESIGNED FOR AN INTEGRAL LIFT ENGINE

## II - PERFORMANCE OF 2-, 3-, AND $3\frac{1}{2}$-STAGE CONFIGURATIONS

by Warren J. Whitney, Harold J. Schum, and Frank P. Behning

Lewis Research Center

## SUMMARY

The performance of the 2-, 3-, and $3\frac{1}{2}$-stage turbine configurations of a $3\frac{1}{2}$-stage fan-drive turbine with a stage loading factor of 4 has been determined. The performance of the first stage (or single stage) configuration was previously investigated and reported. The $3\frac{1}{2}$ stage turbine produced design equivalent work output at design speed with an efficiency of 0.855. This efficiency was within 0.008 of the efficiency predicted value (0.863). This agreement demonstrates the adequacy of the prediction method in the high stage loading factor regime.

At the condition of design work output and design speed, the ratio of equivalent mass flow to design equivalent mass flow was 1.046, 1.042, and 1.046 for the $3\frac{1}{2}$-, 3-, and 2-stage configurations, respectively. The corresponding ratio for the single-stage turbine (obtained in the reference investigation) was 1.049. This indicates that the specific work output - mass flow characteristics of the three stages were closely matched. The excess mass flow occurring at this condition also indicates the desirability of a blading adjustment to increase the stator blade and rotor blade outlet flow angles, and thereby to cause design mass flow to occur at design work output.

The stage work distribution was determined from the $3\frac{1}{2}$-, 2-, and single-stage results. This distribution was first stage, 0.330; second stage, 0.338; third stage, 0.332. This is very close to the design stage work distribution which was 0.333 for all stages.

## INTRODUCTION

In recent years NASA-Lewis Research Center has devoted some effort to the study of engines for vertical and short takeoff and landing (VSTOL) aircraft. One of the types of engines considered for this application is the integral lift engine which is a high by-

pass ratio, quiet turbofan. A preliminary design for an engine of 44 482-newtons (10 000 lb) of thrust was evolved from a parametric computer-programmed study encompassing many engine cycle variations, component arrangements, and operational limitations. The engine had a bypass ratio of 7.47 and a fan pressure ratio of 1.25. A mechanical layout and weight study for this engine, scaled to 55 602 newtons (12 500 lb) of thrust, was made in reference 1.

The characteristics desired for this type of engine are compactness, lightweight, and a high ratio of thrust to engine and fuel weight. A mechanical limitation imposed by noise considerations was that the fan tip speed could not exceed 305 meters per second (1000 ft/sec). As discussed in part I (ref. 2), these requirements resulted in a fan-drive turbine that had to develop its power at a relatively low blade speed. The turbine design selected for this engine (ref. 2) consisted of $3\frac{1}{2}$-stages with a stage loading factor (ratio of change in tangential velocity to blade speed) of 4. As discussed in part I, a stage loading factor of 4 represents a regime where the adequacy of the efficiency estimation procedure has not been confirmed (ref. 2). Yet, if conventional stage loading factors (1.5 to 1.0) had been used, the number of stages would have been 8 to 12.

The details of this design procedure are described in part I. The turbine was a free-vortex design with high aspect ratio and shrouded rotor blades. The performance of the first stage, modified for axial inlet conditions, was determined experimentally in cold air and is included in reference 2.

The first stage of reference 2 was combined with the second stage, third stage, and outlet turning vanes; and the performance was obtained for the 2-, 3-, and $3\frac{1}{2}$-stage configurations. The inlet conditions of pressure and temperature were $1.348\times10^5$ pascals (1.33 atm) and 378 K ($680^\circ$ R). The three-stage configurations were investigated at 70, 80, 90, 100, 110, and 120 percent of design speed. The two-stage turbine performance was determined for 80, 90, 100, 110, 120, and 130 percent of design speed. Each configuration was operated over a wide range of total-pressure ratio at each speed. The basic performance data were obtained as equivalent torque, equivalent mass flow, and average outlet flow angle as functions of turbine total-pressure ratio.

This report presents the additional performance data obtained for the 2-, 3-, and $3\frac{1}{2}$-stage configurations. The data are of general interest in extending reliable performance prediction methods to higher stage loading factor regimes.

## SYMBOLS

A area, $m^2$; $ft^2$

g force-mass conversion constant, 1; 32.174 $ft/sec^2$

h specific enthalpy, J/g; Btu/lb

| | |
|---|---|
| N | rotative speed, rpm |
| P | absolute pressure, $N/m^2$; $lb/ft^2$ |
| R | gas constant for mixture of air and combustion products used in this investigation, 288 J/kg·K; 53.527 (ft·lb)/(lb) $^{o}R$ |
| T | temperature, K; $^{o}R$ |
| U | blade velocity, m/sec; ft/sec |
| V | absolute gas velocity, m/sec; ft/sec |
| W | gas velocity relative to moving blade, m/sec; ft/sec |
| w | mass-flow rate (sum of air and fuel), kg/sec; lb/sec |
| $\alpha$ | absolute gas flow angle measured from axial direction, deg |
| $\overline{\alpha}$ | average absolute gas flow angle at turbine outlet, measured as deviation from axial direction irrespective of sign, used in eq. (2), deg |
| $\beta$ | angle of gas flow relative to moving blade measured from axial direction, deg |
| $\gamma$ | ratio of specific heats, 1.398 for mixture of air and combustion products used in this investigation |
| $\delta$ | ratio of inlet total pressure to U.S. standard sea-level pressure |
| $\epsilon$ | function of $\gamma$, $(0.73959/\gamma)[(\gamma + 1)/2]^{\gamma/(\gamma-1)}$ |
| $\eta$ | efficiency based on total pressure ratio |
| $\theta_{cr}$ | squared ratio of critical velocity at turbine inlet to critical velocity of U.S. standard sea-level air |
| $\tau$ | torque, N-m; ft-lb |

Subscripts:

| | |
|---|---|
| 0 | station at turbine inlet (see fig. 2(a)) |
| 1 | station at stator outlet on velocity diagram |
| 1g | cavity pressure station (see fig. 2(a)) |
| 2 | station at rotor outlet on velocity diagram |
| 3g | cavity pressure station (see fig. 2(a)) |
| 4 | station at outlet of 2-stage turbine (see fig. 2(c)) |
| 5g | cavity pressure station (see fig. 2(a)) |
| 6 | station at outlet of 3-stage turbine (see fig. 2(b)) |
| 7 | station at outlet of $3\frac{1}{2}$-stage turbine (see fig. 2(a)) |

Superscript:

' total state

## TURBINE DESCRIPTION

The details of the turbine blading design were described in reference 2. The turbine velocity diagram is included herein for convenience (fig. 1). The turbine was a free-vortex design with a nearly symmetrical diagram. The flow path for the 2-, 3-, and $3\frac{1}{2}$-stage configurations is shown in figure 2. In all cases inner and outer fairing pieces were provided at the turbine outlet, which were of constant diameter equal to the hub and tip diameters, respectively, at the outlet of the aftermost blade row. A photograph of the rotor assembly is shown in figure 3.

The design requirements for the 3- and $3\frac{1}{2}$-stage configurations are as follows:

| | |
|---|---|
| Equivalent specific work output, $\Delta h/\theta_{cr}$, J/g; Btu/lb | 52.206; 22.445 |
| Equivalent mass flow, $\epsilon w \sqrt{\theta_{cr}}/\delta$, kg/sec; lb/sec | 19.128; 42.17 |
| Equivalent mean blade speed, $U_m/\sqrt{\theta_{cr}}$, m/sec; ft/sec | 66.17; 217.1 |

The requirements for the two-stage turbine are the same except for the equivalent specific work output which is 34.804 joules per gram (14.963 Btu/lb).

## APPARATUS INSTRUMENTATION AND PROCEDURE

The test facility was that described in reference 2. The procedure and instrumentation employed in these tests are nearly the same as those described in reference 2 and are discussed herein only briefly for convenience.

Airflow was measured with a calibrated Dall tube, which is a modified type of venturi meter. The fuel flow-rate to the turbine inlet-air heater was measured with a flat-plate orifice. Both of these flow measuring devices required an upstream pressure, an upstream temperature, and a characteristic differential pressure. The turbine mass flow rate was determined as the sum of these two flows.

The turbine rotational speed was measured with an electronic counter and a square toothed sprocket, which was mounted on the turbine shaft. Turbine output torque was measured with a static load cell on the cradled dynamometer stator. The torque measuring system was calibrated before and after each day's run.

The turbine was instrumented at the stations shown in figure 2. The inlet (station 0) was common to all configurations. The instrumentation at this station consisted of six wall static taps, a rake of five thermocouples, and two total-pressure probes (fig. 4).

The probe total pressure was used for setting inlet conditions, and the inlet total pressure used for the efficiency was calculated from the equation

$$\frac{p'_0}{p_0} = \left[\frac{1}{2} + \sqrt{\frac{1}{4} + \frac{\gamma - 1}{2g\gamma}\left(\frac{w}{p_0 A_0}\right)^2 RT'_0}\right]^{\gamma/(\gamma-1)} \tag{1}$$

as discussed in reference 2.

At station 4, the outlet of the two-stage configuration, the instrumentation consisted of eight wall static-pressure taps and two combination probes (fig. 4). The outlet total pressure was calculated by the equation

$$\frac{p'_4}{p_4} = \left[\frac{1}{2} + \sqrt{\frac{1}{4} + \frac{\gamma - 1}{2g\gamma}\left(\frac{w}{P_4 A_4}\right)^2 \frac{RT'_4}{\cos^2 \bar{\alpha}_4}}\right]^{\gamma/(\gamma-1)} \tag{2}$$

which is the same as that used for the inlet except that the flow area is adjusted by the deviation angle $\bar{\alpha}_4$. The angle $\bar{\alpha}_4$ is the average deviation from the axial direction, irrespective of sign. This angle was measured at the area center radii of five equal concentric annular areas.

At stations 6 and 7 the static pressure was measured with eight wall taps (see fig. 4). The flow angle was measured at the area center radii of four equal concentric annular areas. The equation used to calculate the outlet total pressure at stations 6 and 7 is the same as that used for station 4 (eq. (2)). The turbine outlet total temperature ($T'_4$, $T'_6$, or $T'_7$) was derived from the inlet total temperature $T'_0$, torque, speed, and mass flow. At the stations 1g, 3g, and 5g static pressure was measured in the outer cavities (see fig. 2(b)) with two taps installed at each station.

The observed data are presented for each configuration as curves of equivalent torque, equivalent mass flow, and average outlet flow angle as functions of total pressure ratio for the various speeds. The performance maps were constructed from plots of equivalent specific work output and equivalent mass-flow-speed parameter as functions of total pressure ratio.

The inlet total pressure and total temperature were maintained constant at $1.348 \times 10^5$ pascals (1.33 atm) and 378 K (680° R). The 3- and $3\frac{1}{2}$-stage configurations were investigated at 70, 80, 90, 100, 110, and 120 percent of design speed. The 2-stage turbine performance was determine for 80, 90, 100, 110, 120, and 130 percent of design speed. Each configuration was operated over a wide range of total-pressure ratio at each speed.

## RESULTS AND DISCUSSION

This section includes the following: a description of the performance of the three stage groupings, a discussion of the effect of measurement error on efficiency, a discussion of stage work distribution at the condition of design work extraction for the $3\frac{1}{2}$-stage configuration, a comparison of predicted and experimental efficiencies for the stage groupings and individual stages, and a discussion of a possible blading adjustment.

### Stage Grouping Performance

Two-stage configuration. - The data obtained for the two-stage configuration are shown as equivalent mass flow, equivalent torque, and average outlet flow angle as functions of total-pressure ratio in figures 5 to 7. Figure 5 shows that choking does not occur for the range of pressure ratios investigated, and figure 6 shows that limiting loading is not approached at any of the speeds. This is the expected result for a turbine employing low relative Mach numbers (fig. 1). In figure 8 the data of figures 5 to 7 are combined to obtain the performance map. The 2-stage turbine developed design work output at a pressure ratio of 1.701, corresponding to an efficiency of 0.853. The equivalent mass flow at this condition was 20.008 kilograms per second (44.10 lb/sec) or 1.046 times design. The corresponding mass flow for the single-stage turbine (ref. 2) at design work extraction was 1.049 times the design value. Thus, the mass-flow-work extraction characteristic of the 2-stage turbine closely duplicates that of the single-stage configuration. The average outlet flow angle (fig. 7) was $32.0^{\circ}$ at a pressure ratio of 1.701 compared with a mean radius design flow angle of $36.85^{\circ}$.

Three-stage configuration. - The basic data obtained for the 3-stage turbine are shown in figures 9 to 11. The turbine was near choking at the highest pressure ratios for all speeds (fig. 9). The torque curves of figure 10 show no indication of limiting loading. The performance map was constructed from the data of figures 9 to 11 and is shown in figure 12. Equivalent design work output was obtained for the 3-stage turbine at a total pressure ratio of 2.295 corresponding to an efficiency of 0.853.

The mass-flow at this condition was 19.94 kilograms per second (43.96 lb/sec) or 1.042 of design. Thus the 3-stage turbine has a mass flow work extraction characteristic that is very close to that of the single-stage and 2-stage configurations. The outlet flow angle of the 3-stage turbine was $36.2^{\circ}$ at design work extraction ($P'_0/P'_6 = 2.295$) as compared with the design mean radius flow angle of $36.85^{\circ}$ (fig. 11).

Three and a half stage turbine. - The performance data for the $3\frac{1}{2}$-stage turbine are shown in figures 13 to 15. The $3\frac{1}{2}$-stage turbine was operated at higher pressure-ratios (fig. 13) than was the 3-stage (fig. 9) and therefore appears to be more definitely choked.

This effect is also shown in the torque curves of figure 14 where the $3\frac{1}{2}$-stage turbine is shown to be near limiting-loading at the highest pressure ratio, whereas the pressure ratio range covered for the 3-stage turbine (fig. 9) was not great enough to show this trend. The overall performance map constructed from the data of figures 13 to 15 is shown in figure 16.

The $3\frac{1}{2}$-stage turbine developed design equivalent work output at a pressure ratio of 2.290, with a corresponding efficiency of 0.855. The equivalent mass flow at this condition was 20.012 kilograms per second (44.12 lb/sec) or 1.046 times the design mass flow. Thus, the mass flow at design work extraction was very closely matched for all the stage groupings.

The efficiency and mass-flow results for the stage groupings including the single-stage results of reference 2, are summarized in table I.

TABLE I. - EFFICIENCY AND

MASS FLOW RESULTS

| Number of turbine stage | Experimental efficiency | Mass flow, fraction of design |
|---|---|---|
| 1 | 0.858 | 1.049 |
| 2 | .853 | 1.046 |
| 3 | .853 | 1.042 |
| $3\frac{1}{2}$ | .855 | 1.046 |

## Effect of Measurement Error on Efficiency

In table I it can be noted that the efficiency of the $3\frac{1}{2}$ stage turbine was 0.855 and that of the 3-stage turbine was 0.853. The fact that the 3-stage was lower (even though only slightly) indicates that one of these efficiencies must be in error.

The accuracy of the turbine efficiency depends on the measurements of torque, speed, mass flow, static pressure, and outlet flow angle. Of these quantities, the measurement of outlet flow angle was the most probable source of efficiency error. The effect of a $1^{\circ}$ change in the outlet angle $\overline{\alpha}$ was determined at the condition of design work output for the three stage groupings and for the single-stage turbine of reference 2. These results are listed in table II. A $1^{\circ}$ error in $\overline{\alpha}$ affects the

TABLE II. - EFFECT OF MEASUREMENT

ERROR ON EFFICIENCY

| Number of turbine stages | Efficiency change for $\Delta\overline{\alpha} = 1^{\circ}$ | Maximum efficiency error due to outlet pressure transducer |
|---|---|---|
| 1 | 0.015 | 0.0083 |
| 2 | .0054 | .0049 |
| 3 | .0048 | .0040 |
| $3\frac{1}{2}$ | .00037 | .0047 |

efficiency of the 2- and 3-stage turbines by about 0.005 but has only a slight effect on the efficiency of the $3\frac{1}{2}$-stage turbine.

The outlet static-pressure measurement is another source of error because of the inaccuracy of the pressure transducers. The effect on efficiency of a maximum error in outlet static pressure are included in table II. These effects were also determined at design work output using the maximum transducer error (1/4 percent of the maximum transducer operating pressure). The tabulated maximum efficiency error due to transducer error was between 0.004 and 0.005 for the 2-, 3-, and $3\frac{1}{2}$-stage configurations. Even this amount of error is contingent on the two outlet absolute pressure transducers being in error in the same direction (either too high or too low) simultaneously.

It is felt, therefore, that the most likely cause of the untenable efficiency ranking of the 3- and $3\frac{1}{2}$-stage configurations is due to the error in determining the outlet flow angle. The outlet flow angle error may result partly from installation error in mounting the probe and actuator and partly from the averaging method of reducing the many angle readings into one effective average flow angle. The effects on efficiency shown in table II would also indicate that the $3\frac{1}{2}$-stage results are the most reliable of the four configurations. The effect of angle error on efficiency is over 10 times as great for the 3-stage turbine as it is for the $3\frac{1}{2}$-stage configuration.

## Stage Work Distribution

The turbine was equipped with two cavity pressure measuring taps each at stations 1g, 3g, and 5g (fig. 2). The intent of including the cavity pressures was to establish the stage work distribution. This method was not satisfactory, however, for two reasons: (1) The gradient of cavity-pressure-to-inlet-pressure ratio against specific work output

was very small, such that a small error in cavity pressure resulted in a large change in specific work output. (2) There were only two cavity pressure taps at each location and one or more of these six were frequently inoperative, thus, reliable cavity pressures could not be determined for many of the data points.

The mass-flow measurement was, therefore, used to indicate the distribution of work among the three stages using the $3\frac{1}{2}$- 2-, and 1-stage configurations. The mass-flow value for design work extraction for the $3\frac{1}{2}$-stage configuration (fig. 17) was 20.012 kilograms per second (44.12 lb/sec). This mass-flow value was used to denote the specific work output of the 2- and 1-stage configurations in figure 17. The stage work distributions are shown in table III.

TABLE III. - STAGE WORK DISTRIBUTION

| Stage | Specific work output, J/g; Btu/lb | Fraction of total work output |
|---|---|---|
| 1 | 17.212; 7.40 | 0.330 |
| 2 | 17.654; 7.59 | .338 |
| 3 | 17.340; 7.455 | .332 |

The stage work distribution was very close to design, in which each stage developed 0.333 of the total work output.

## Comparison with Predicted Efficiencies

Stage grouping efficiency. - The efficiencies of the three turbine configurations at the condition of design work extraction are compared with the efficiency predicted by using reference 3 in table IV. The predicted overall efficiencies of the stage groupings were obtained by using the design stage work outputs and predicted stage efficiencies of the individual stages. The stage efficiencies were determined from figure 18, which is derived from reference 3 and is a reproduction of figure 1(a) of reference 2. The overall pressure ratio was determined from the product of the stage pressure ratios. Thus the overall efficiency of the stage groupings includes the effect of reheat. In the cases where the turbines had outlet turning vanes, the outlet turning vane loss was estimated by using figure 203(b) of reference 4, and this loss was then factored into the overall pressure ratio. The turbines from references 5 and 6 are included in the comparison of table IV.

TABLE IV. - COMPARISON OF PREDICTED

AND EXPERIMENTAL EFFICIENCIES

| Number of turbine stages | Efficiency | | Average stage loading factor |
|---|---|---|---|
| | Experimental | Predicted (ref. 3) | |
| 2 | 0.853 | 0.869 | 4 |
| 3 | .853 | .869 | 4 |
| $3\frac{1}{2}$ | .855 | .863 | 4 |
| [a]3 | .885 | .891 | 3 |
| [b]$4\frac{1}{2}$ | .852 | .843 | 5 |

[a]From ref. 5.

[b]From ref. 6.

Both the 2- and 3-stage configurations had an experimental efficiency of 0.853, which in both cases was 0.016 lower than the predicted efficiency. The results obtained with the $3\frac{1}{2}$-stage turbine were considered the most reliable of the three configurations. It had an efficiency of 0.855 or 0.008 lower than the predicted value of 0.863. This result is similar to that of reference 5 where the experimental efficiency was 0.006 lower than the predicted value. The $4\frac{1}{2}$-stage turbine of reference 6 had an experimental efficiency 0.009 higher than the predicted value. In summary, the experimental efficiencies of the $3\frac{1}{2}$-stage turbine and the two reference turbines were within 0.01 of the predicted value. This agreement demonstrates the adequacy of the prediction method for high-stage-loading-factor turbines.

Second and third stage efficiencies. - In addition to the stage grouping efficiencies, it is also possible to determine the individual stage efficiencies from the test results described herein and from those of reference 2. This was done for the condition of design 3-stage work extraction using the results from the $3\frac{1}{2}$-, 2-, and 1-stage configurations. The pressure ratios of the 2- and 1-stage configurations were then determined at the reference mass flow (fig. 17), 20.012 kilograms per second (44.12 lb/sec). The stage pressure ratios for the second and third stages could then be isolated, and the stage efficiencies determined. These efficiencies were of interest because the prediction curve (fig. 18) indicates a substantial difference between the efficiency of a first stage and that of an intermediate stage at high stage loading factors. The results of this procedure are summarized in table V. The two aft stages of the reference 5 turbine are included in the comparison. In general the agreement is good between the experimental points and the predicted efficiency. The greatest deviation was 0.017 for the second stage of the reference turbine.

TABLE V. - COMPARISON OF EXPERIMENTAL

AND PREDICTED STAGE EFFICIENCY

| Stage | Stage efficiency determined from experimental results | Predicted stage efficiency[b] | Stage loading factor |
|---|---|---|---|
| 2 | 0.837 | 0.849 | 4 |
| 3 | .856 | .849 | 4 |
| [a]2 | .846 | .863 | 3.5 |
| [a]3 | .923 | .913 | 1.64 |

[a]From ref. 5.

[b]See ref. 3 and fig. 18.

### Blading Adjustment

The velocity diagram of reference 2, which was constructed from the experimental results, indicated that the flow out of the stator and rotor was underturned by $1.4^{\circ}$ and $1.7^{\circ}$ respectively. It was suggested in reference 2 that resetting the blades would cause design mass flow to occur at design specific work output. It was felt that this would improve the performance at design work output by causing the peak efficiency to fall closer to the design point. This appears to be equally applicable for the 2-, 3-, and $3\frac{1}{2}$-stage configurations. The mass-flow - speed characteristics for the 2-, 3-, and $3\frac{1}{2}$-stage configurations are similar to that of the single-stage turbine, with 0.04 or more excess mass flow occurring at the design work output-design speed condition. Also, the magnitude of the peak efficiency and its relation to the design point (figs. 8, 12, and 16) are similar to that obtained for the single-stage turbine.

## SUMMARY OF RESULTS

The cold air performance of the 2-, 3-, and $3\frac{1}{2}$-stage configurations of a $3\frac{1}{2}$-stage fan-drive turbine with a stage loading factor of 4 has been determined. The pertinent results are as follows:

1. The $3\frac{1}{2}$-stage turbine produced design equivalent work output at an efficiency of 0.855. The efficiency estimated for this turbine from a reference prediction method was 0.863.

2. At the condition of design work extraction at design speed the ratio of equivalent mass flow to design equivalent mass flow was 1.046, 1.042, and 1.046 for the $3\frac{1}{2}$-, 3-, and 2-stage configurations, respectively. The corresponding ratio for the single-stage turbine, obtained in the reference investigation, was 1.049. This indicates that the specific work-mass flow characteristics were closely matched for the three stages.

3. The stage work-distribution was determined from the $3\frac{1}{2}$-, 2-, and single-stage results to be first stage, 0.330; second stage, 0.338; and third stage, 0.332. The design distribution was 0.333 for all stages.

4. The excess mass flow occurring at design speed and design work output indicated the desirability of a blading geometry adjustment to increase the stator blade and rotor blade outlet flow angles and thereby to cause design mass flow to occur at design specific work output.

5. The validity of the performance prediction method for turbines with high stage loading factor was demonstrated by the fact that the $3\frac{1}{2}$-stage efficiency was predicted within 0.008.

Lewis Research Center,
National Aeronautics and Space Administration,
Cleveland, Ohio, October 26, 1976,
505-04.

## REFERENCES

1. Pratt, W.; Leto, A.; and Schaefer, R.: Integral Lift Engine Preliminary Design. (CW-WR-71-091F, Curtiss-Wright Corp.; NAS3-14327) NASA CR-120838, 1971.

2. Whitney, Warren J.; Schum, Harold J.; and Behning, Frank P.: Cold-Air Investigation of a $3\frac{1}{2}$-Stage Fan-Drive Turbine With a Stage Loading Factor of 4 Designed for an Integral Lift Engine. I - Turbine Design and Performance of First Stage. NASA TM X-3289, 1975.

3. Stewart, Warner L.; and Glassman, Arthur J.: Analysis of Fan-Turbine Efficiency Characteristics in Terms of Size and Stage Number. NASA TM X-1581, 1968.

4. Johnsen, Irving A.; and Bullock, Robert O., eds.: Aerodynamic Design of Axial-Flow Compressors. Revised, NASA SP-36, 1965.

5. Wolfmeyer, G. W.; and Thomas, M. W.: Highly Loaded Multi-Stage Fan Drive Turbine - Performance of Initial Seven Configurations. NASA CR-2362, 1974.

6. Walker, N. D.; and Thomas, M. W.: Experimental Investigation of a $4\frac{1}{2}$-Stage Turbine with Very High Stage Loading Factor. II - Turbine Performance. NASA CR-2363, 1974.

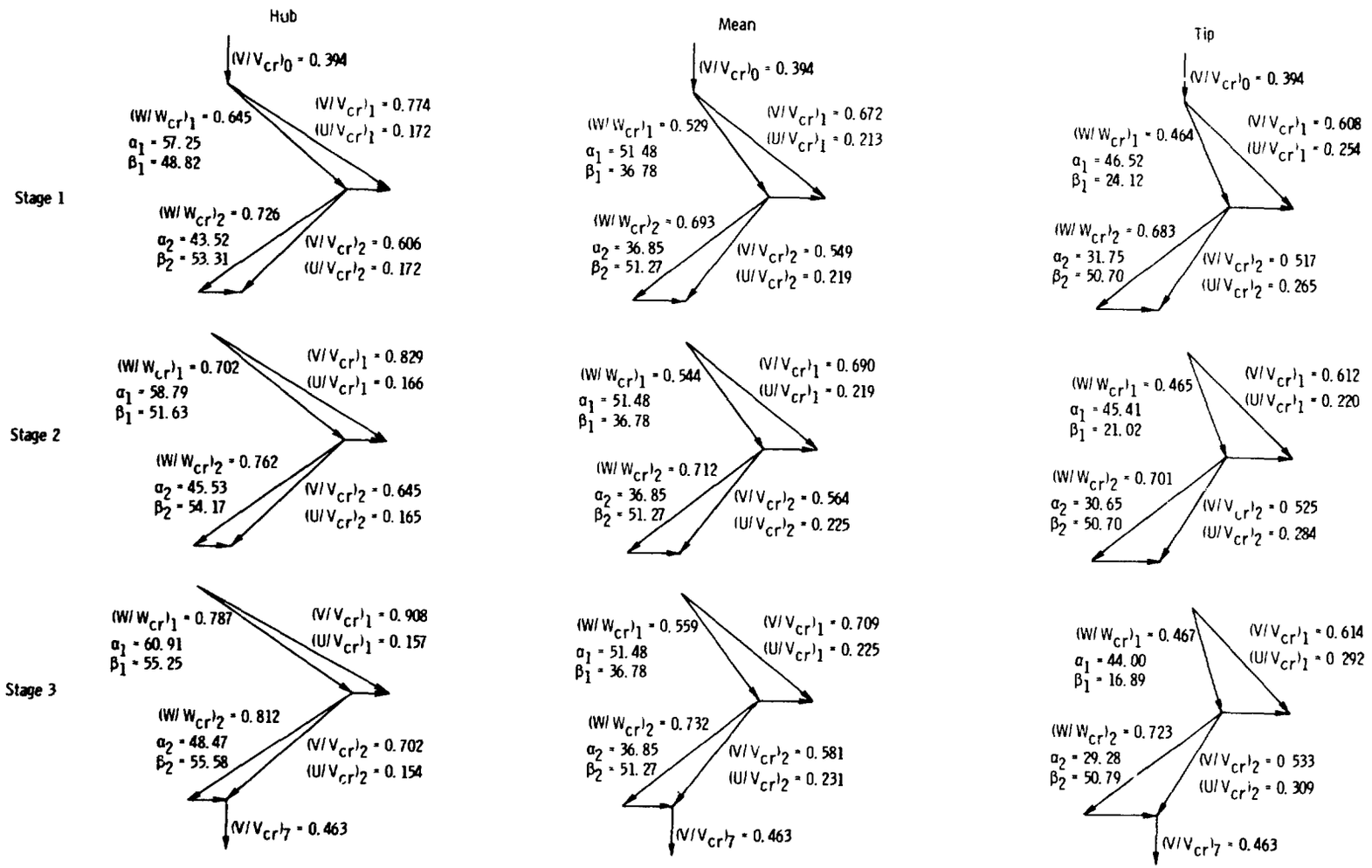


Figure 1. - Velocity diagram of $3\frac{1}{2}$-stage turbine.

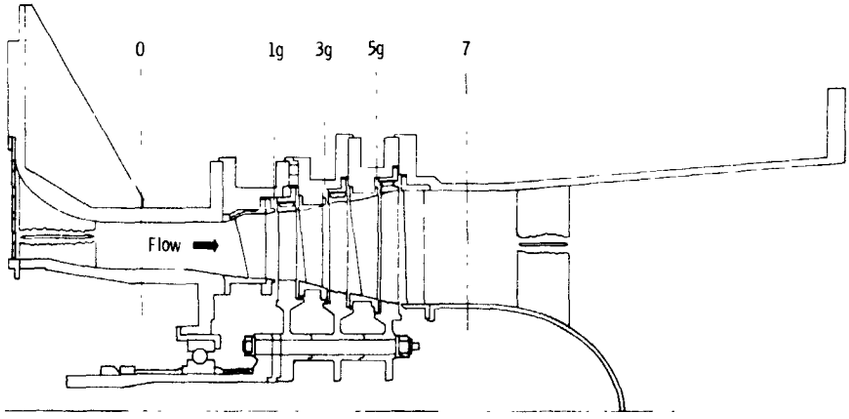


(a) $3\frac{1}{2}$-Stage configuration.

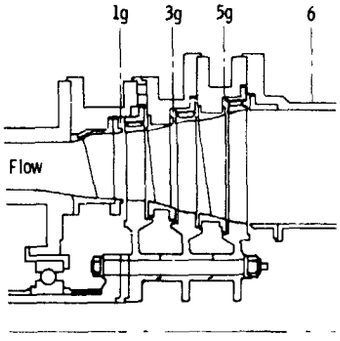


(b) Three-stage configuration.

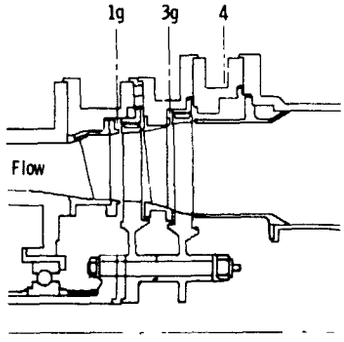


(c) Two-stage configuration.

Figure 2. - Turbine test sections.

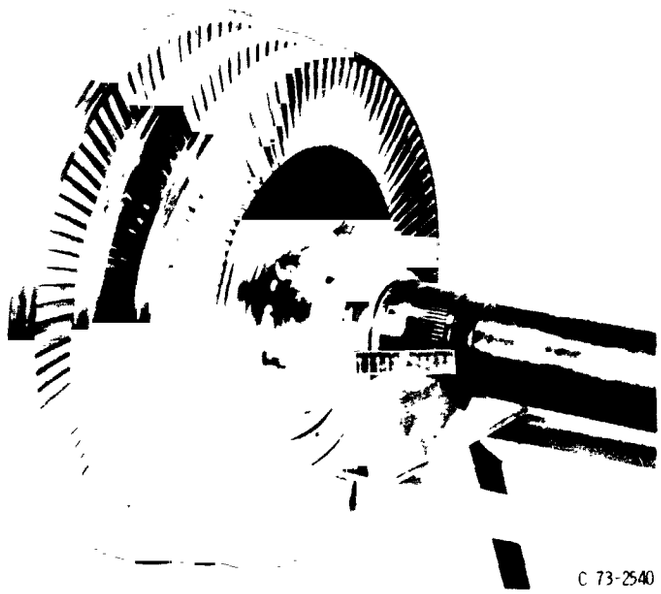


Figure 3. - Rotor assembly for 3½-stage turbine.

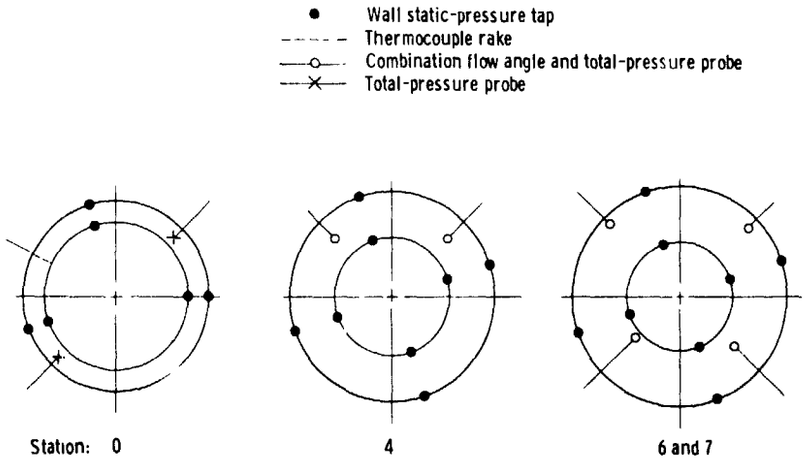


Figure 4. - Turbine instrumentation.

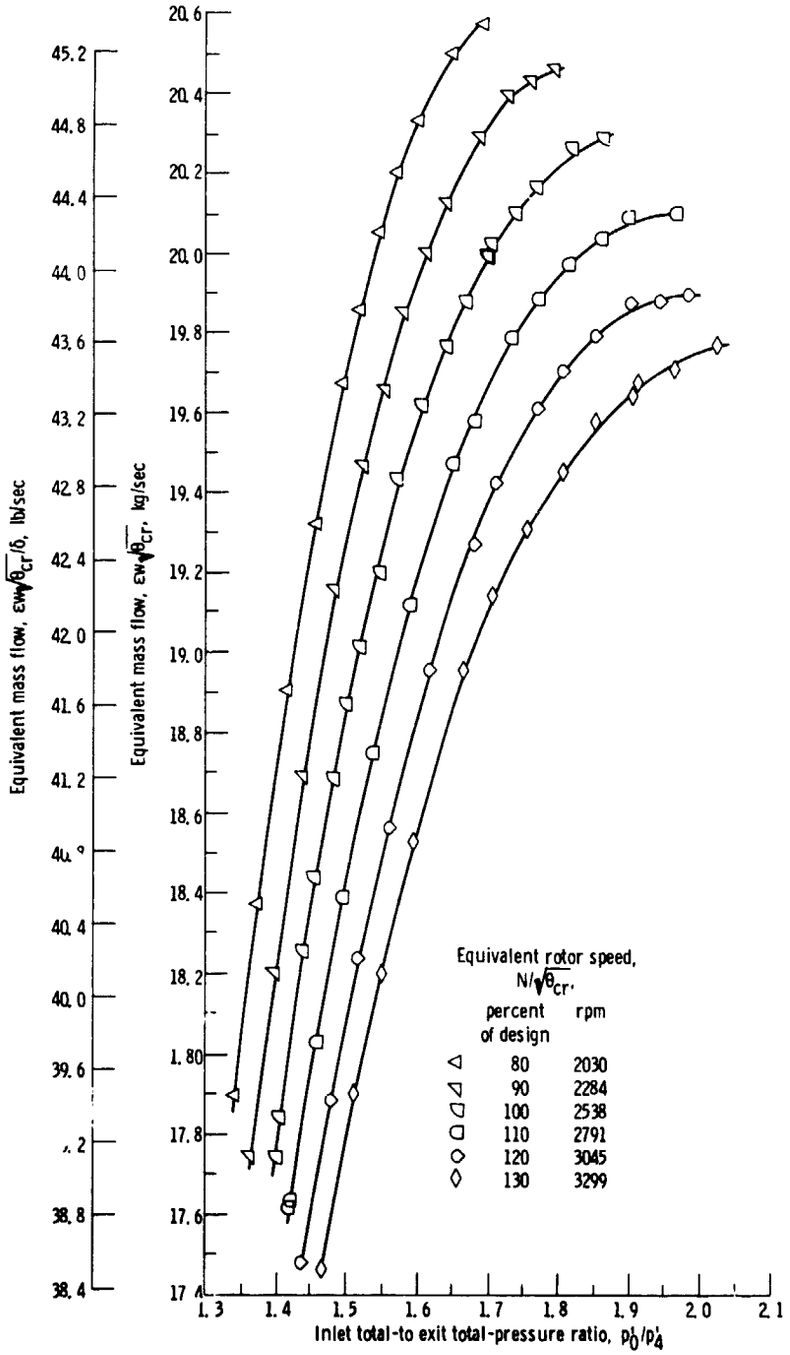


Figure 5. - Variation of equivalent mass flow with total-pressure ratio for various speeds of two-stage turbine.

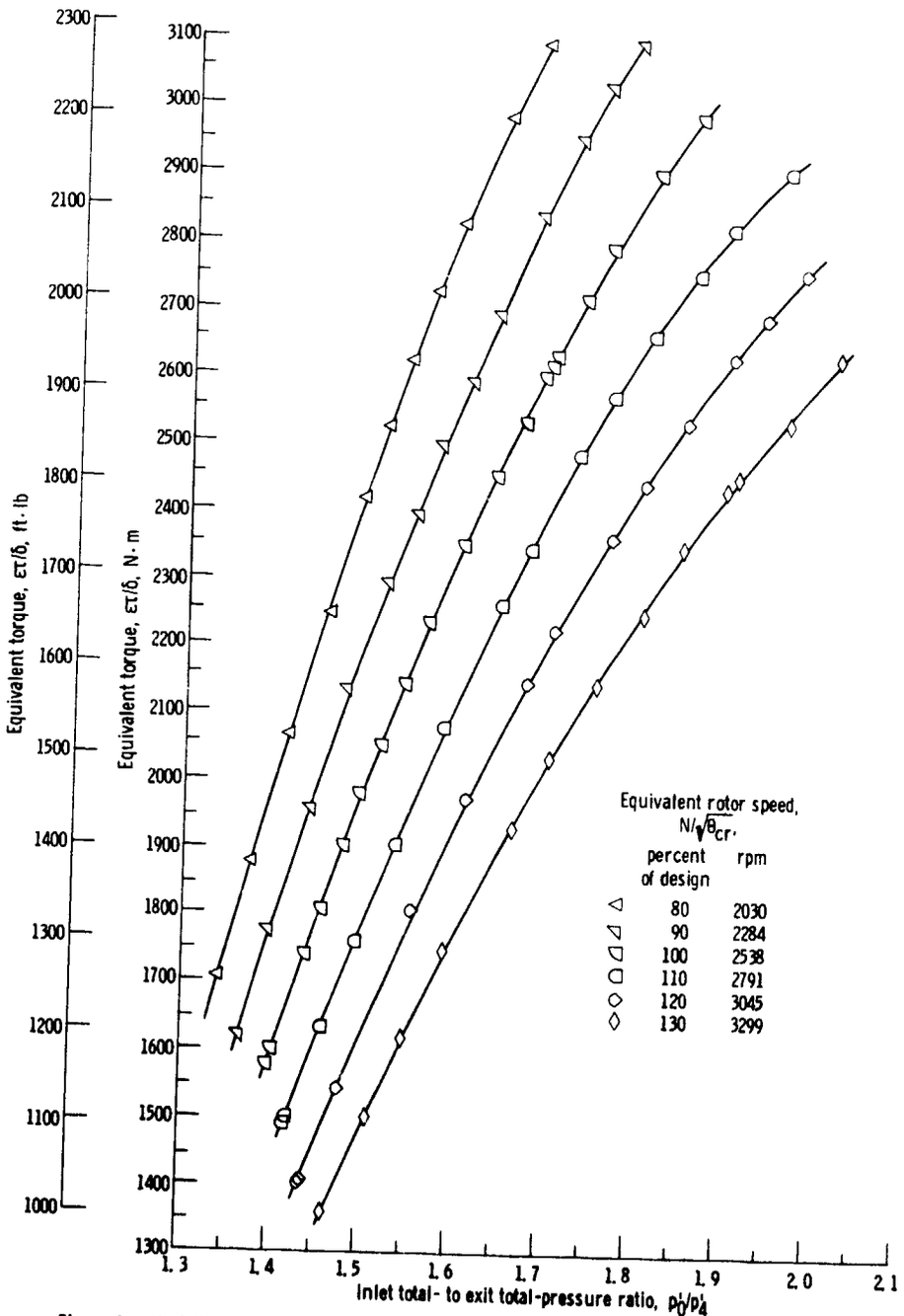


Figure 6. - Variation of equivalent torque with total-pressure ratio for various speeds of 2-stage turbine.

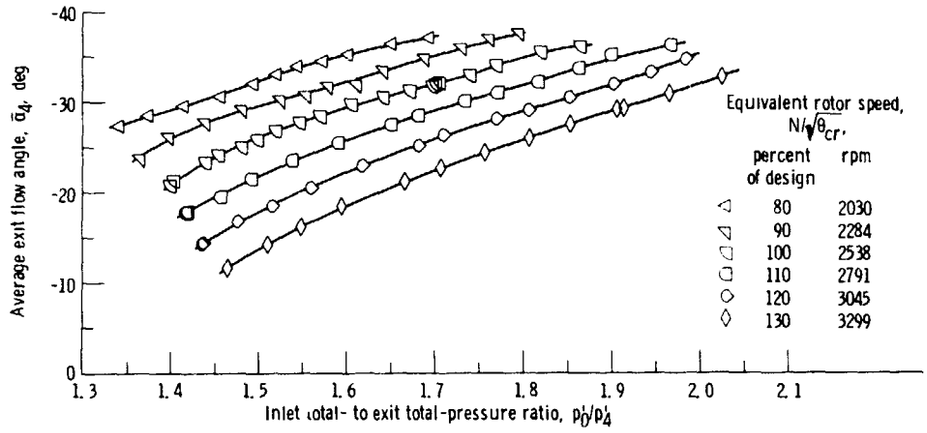


Figure 7. - Variation of average outlet flow angle of 2-stage turbine.

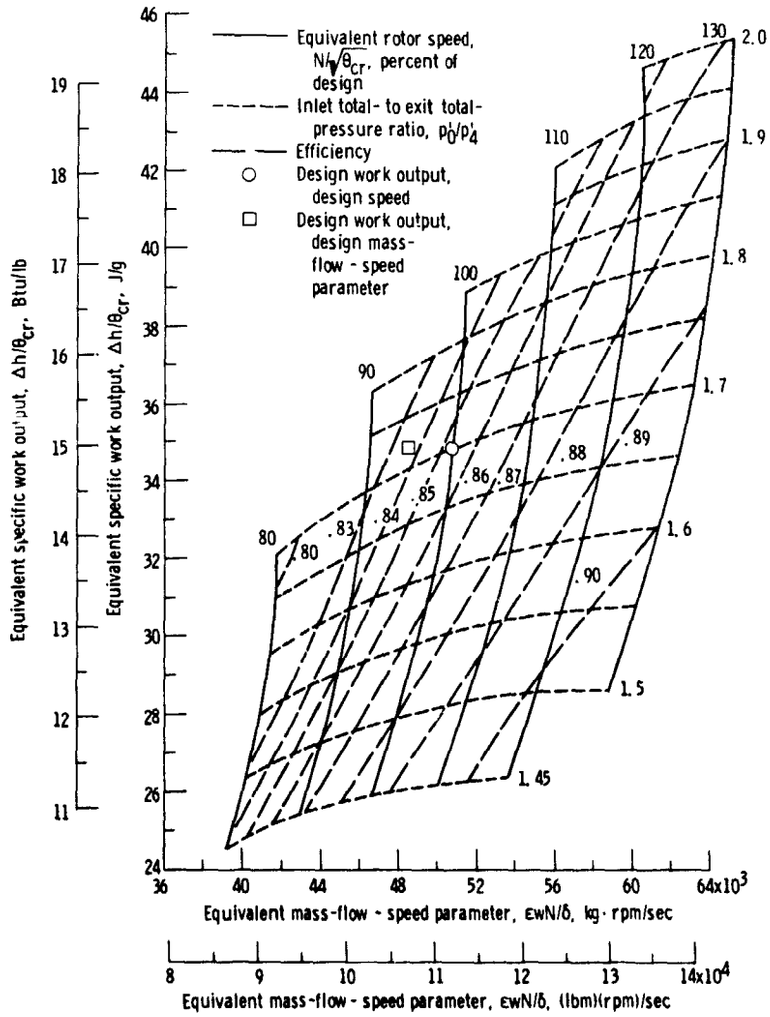


Figure 8. - Performance map for 2-stage turbine.

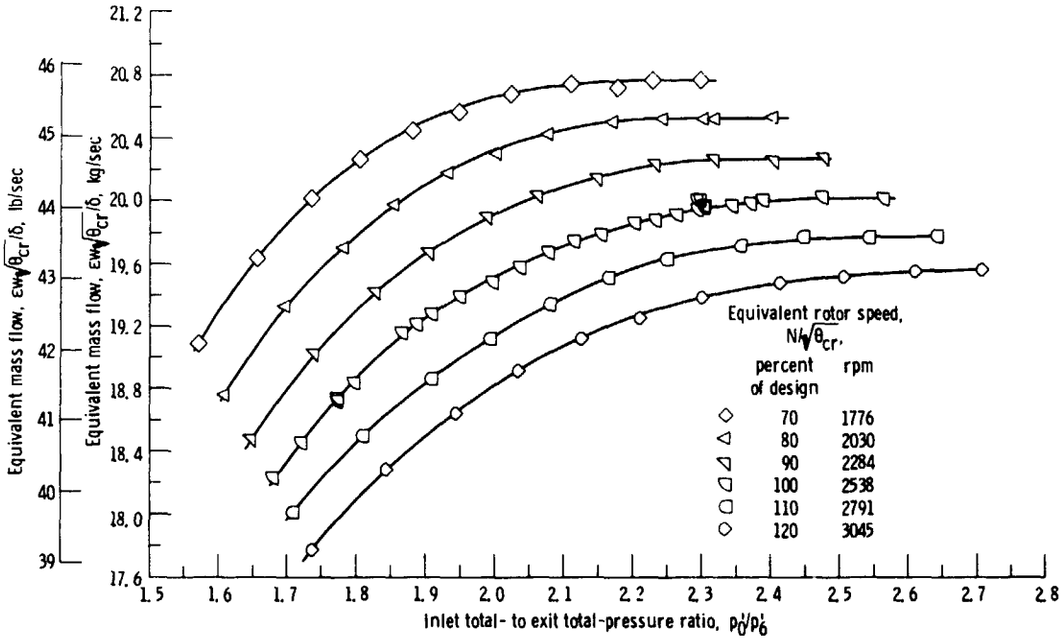


Figure 9. - Variation of equivalent mass-flow with total-pressure ratio for various speeds of 3-stage turbine.

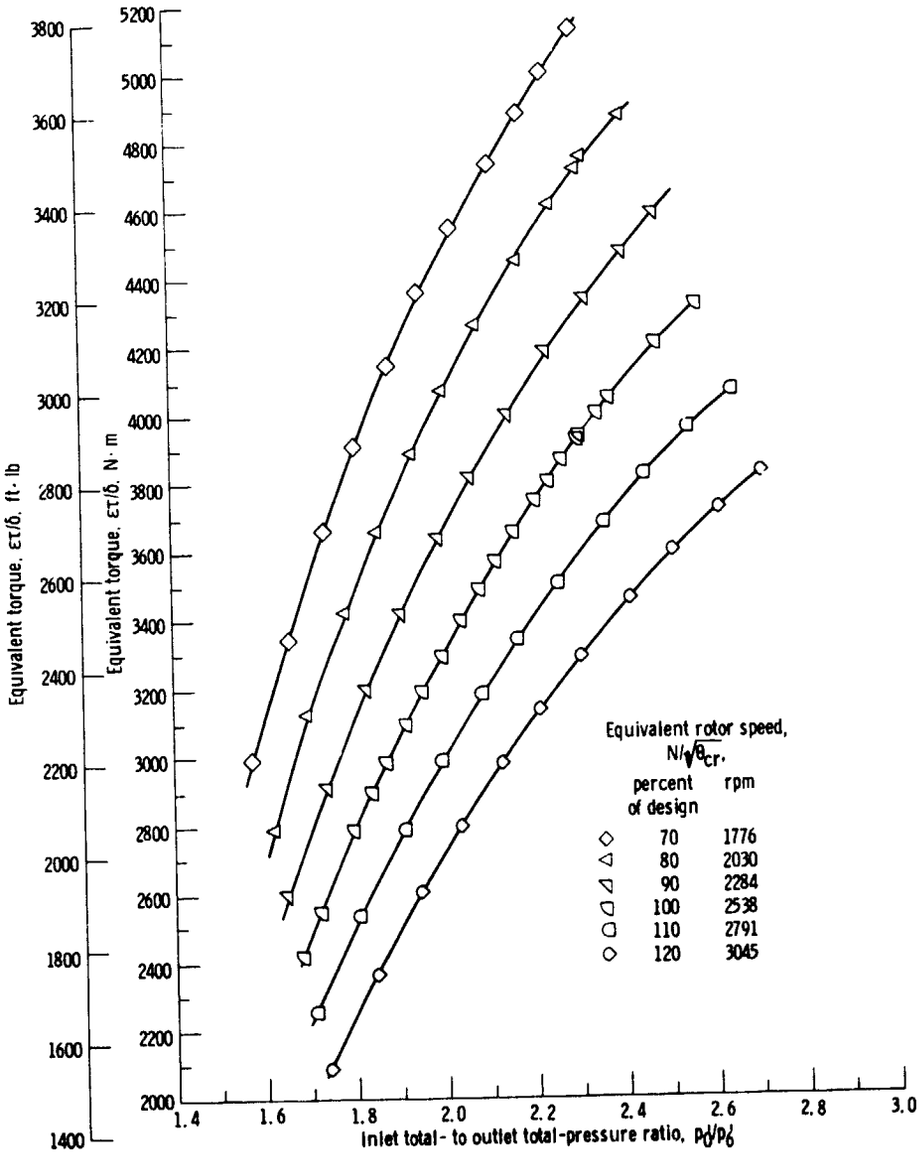


Figure 10. - Variation of equivalent torque with total-pressure ratio for various speeds of 3-stage turbine.

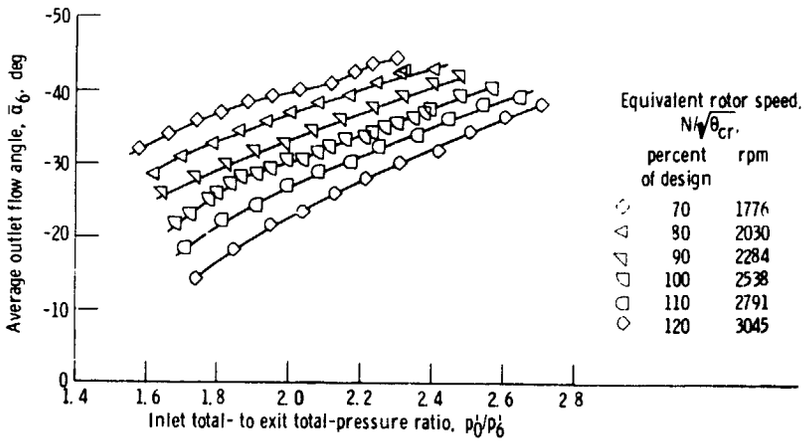


Figure 11. - Variation of average outlet flow angle of 3-stage turbine.

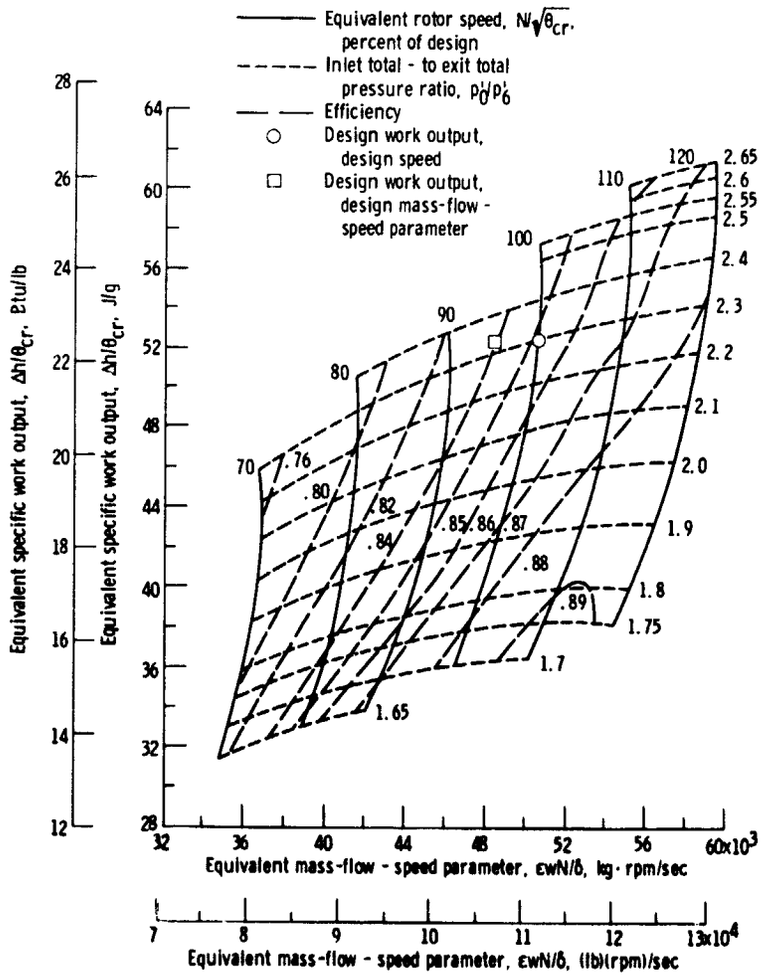


Figure 12. - Performance map for 3-stage turbine.

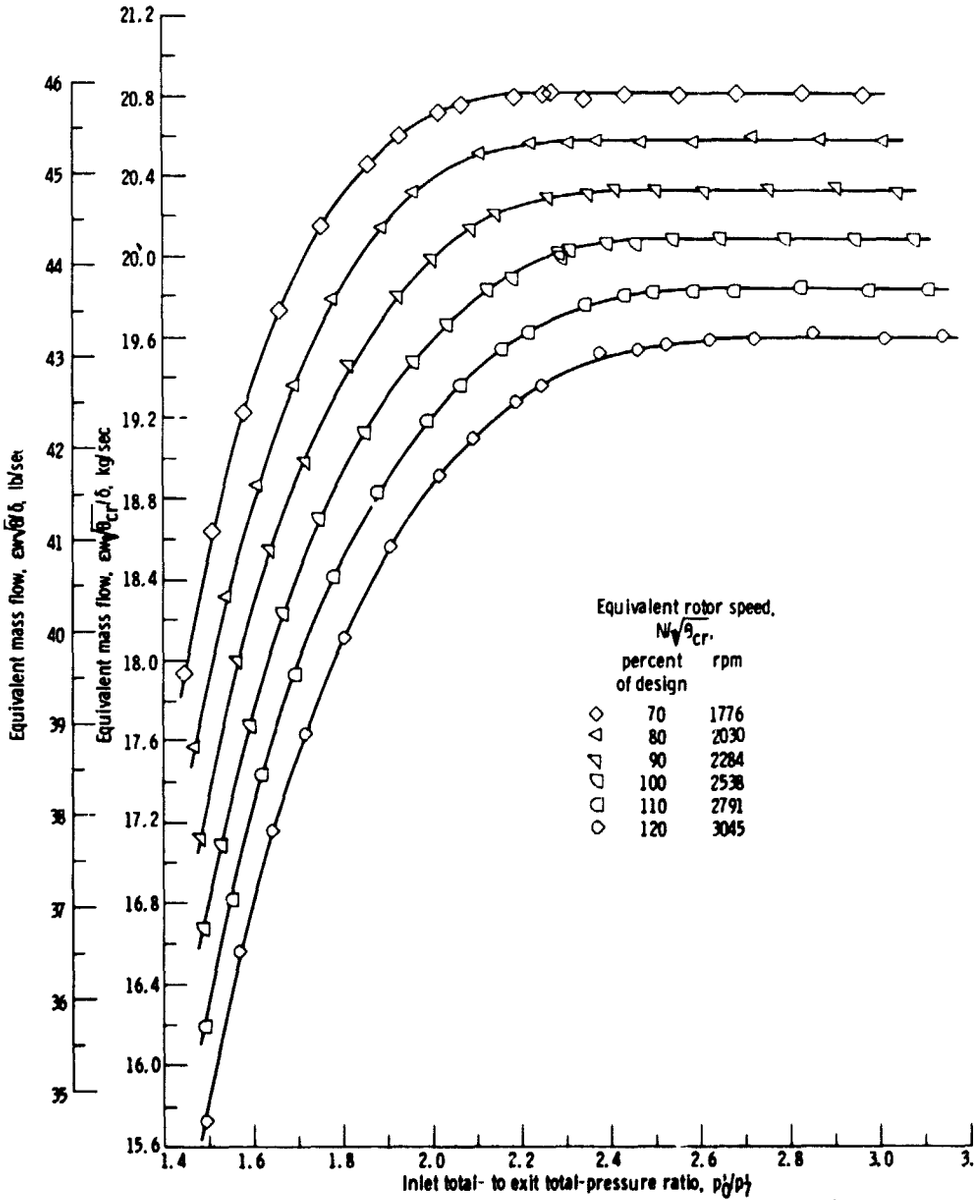


Figure 13. - Variation of equivalent mass flow with total-pressure ratio for various speeds of $3\frac{1}{2}$-stage turbine.

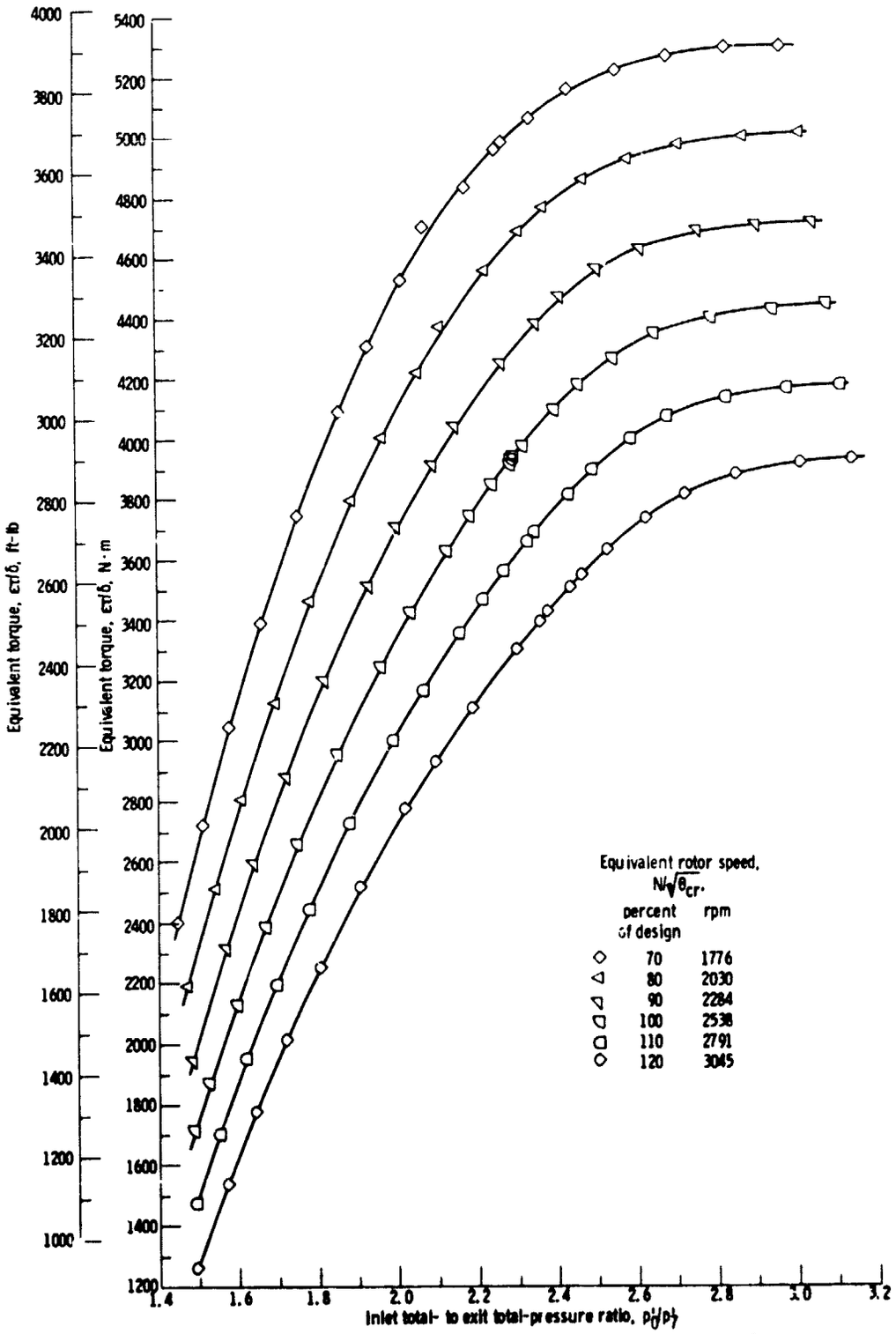


Figure 14. - Variation of equivalent torque with total-pressure ratio for various speeds of $3\frac{1}{2}$-stage turbine.

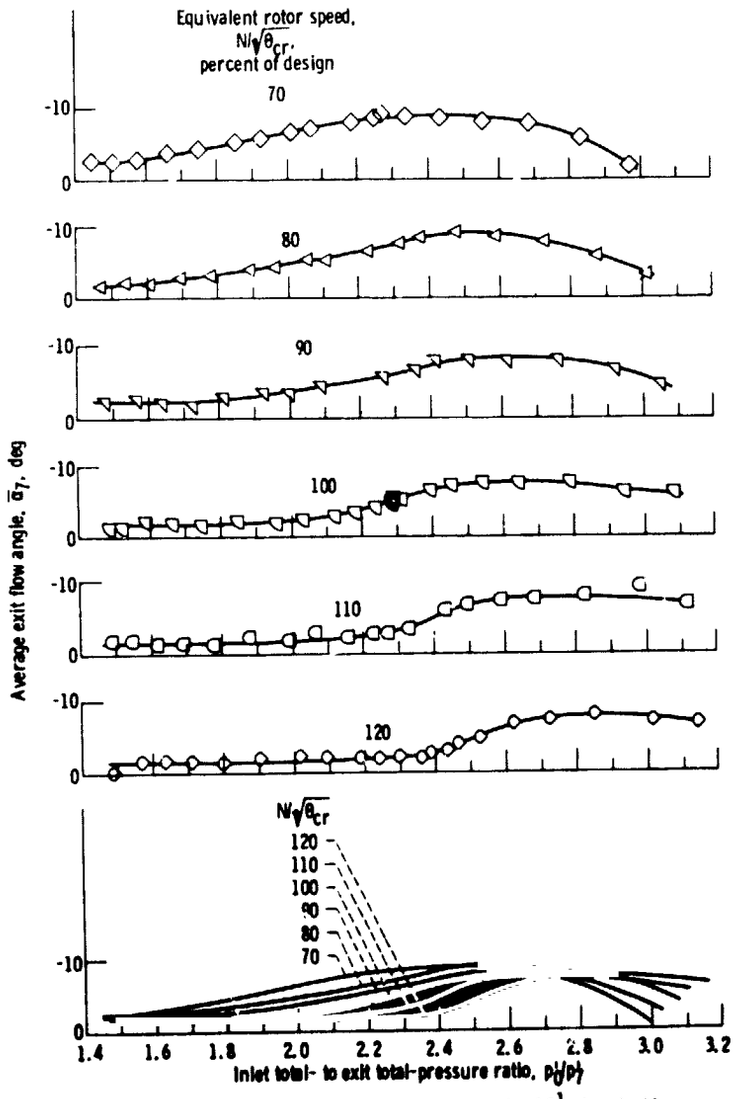


Figure 15. - Variation of average outlet flow angle of $3\frac{1}{2}$-stage turbine.

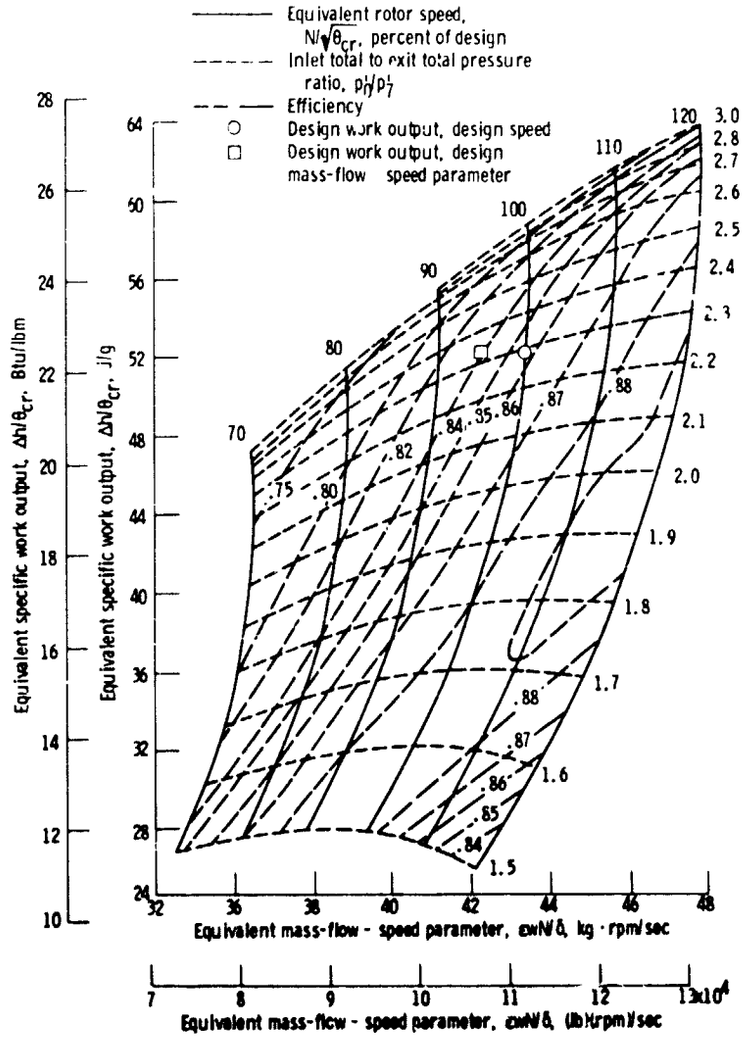


Figure 16. - Performance map for $3\frac{1}{2}$-stage turbine.

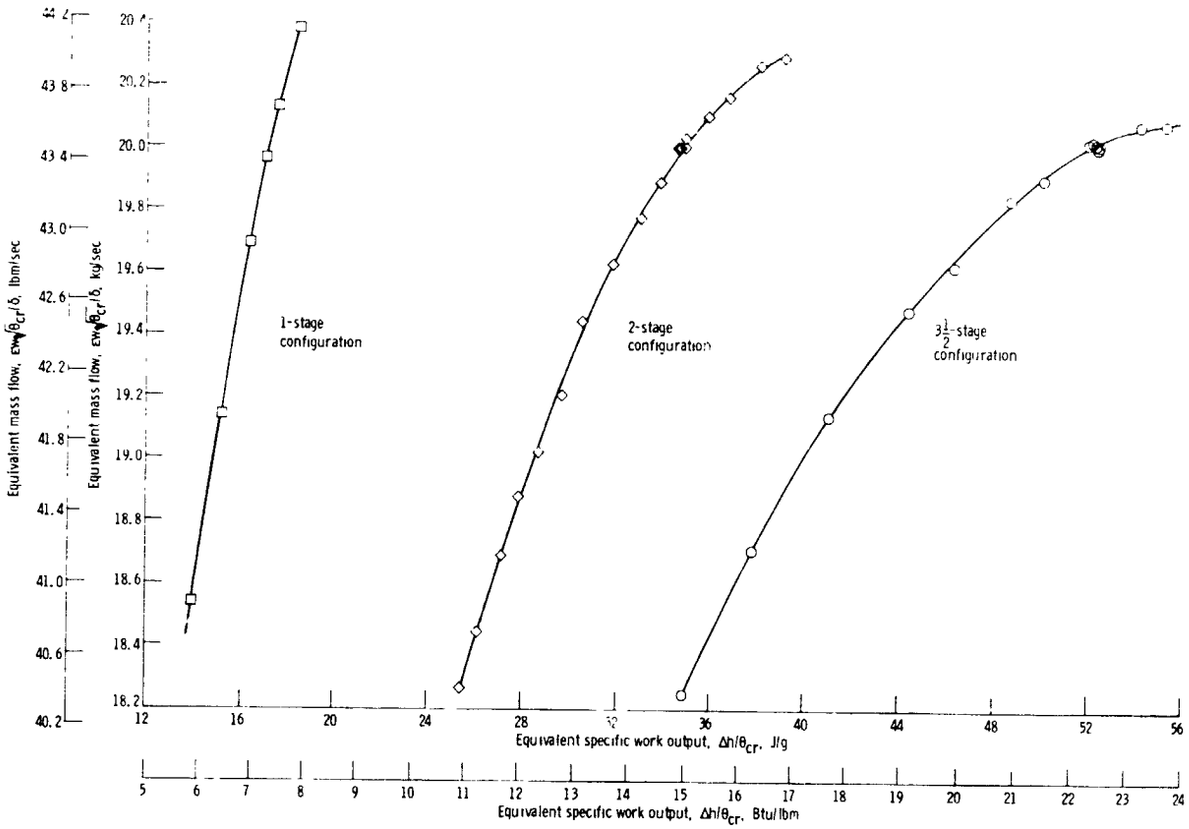


Figure 17 - Variation of equivalent specific work output with equivalent mass flow for $3\frac{1}{2}$-, 2-, and 1-stage configurations. Used to determine stage work distribution

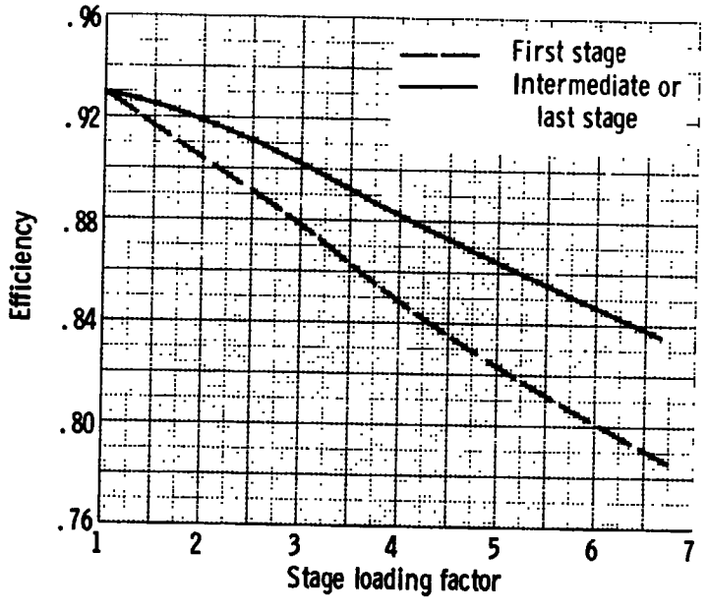


**Figure 18. - Variation of stage efficiency with stage loading factor.**